Structural and Mechanical Properties Investigations in an Ultrafine-Grained 6063-T1 Aluminum Alloy Produced by Severe Plastic Deformation

NICOLAE SERBAN[1]*, DOINA RADUCANU, VASILE-DANUT COJOCARU, MIHAI BUTU
University Politehnica of Bucharest, Materials Science and Engineering Faculty, 313 Spl. Independenţei, 060042, Bucharest, Romania

Severe plastic deformation (SPD) is a manufacturing technique for producing bulk ultrafine grained materials and nanomaterials, the advanced grain refinement obtained by SPD substantially improving structural and physico-mechanical characteristics for the processed material. Equal-channel angular pressing (ECAP), the main SPD technology, entails pressing test samples through a die containing two channels equal in cross section and intersecting at a certain angle. The billet theoretically deforms by simple shear and retains the same cross sectional area to allow repeated pressings for several cycles. A commercial Al-Mg-Si alloy (6063-T1) was investigated in this study. As-received 6063-T1 alloy was firstly analyzed in OES and XRD tests. The specimens were subsequently processed at ambient temperature for a number of passes up to nine (one, three, six and nine ECAP passes), using a die channel angle of 100°. After ECAP, samples were cut from each specimen (ECAP treated and as-received) and prepared for microstructural investigations (SEM) and mechanical testing (compression and microhardness tests, fracture surfaces analysis). Furthermore, multiple correlations between ECAP processing parameters and the resulting microstructure and mechanical properties for the ECAP treated 6063-T1 alloy were also determined.

Keywords: ultrafine-grained materials, aluminum alloys, severe plastic deformation, equal-channel angular pressing

Severe plastic deformation (SPD) research activity has increased extremely over the past decade, due to many interesting and remarkable properties that can be achieved in bulk materials by SPD processing [1-3]. More recently, SPD was in the spotlight of researchers and academics around the world as being a technique capable of producing fully dense and bulk submicrocrystalline and nanocrystalline materials. Conventionally, SPD processing may be defined as those metal-forming procedures in which a very high strain is imposed on a bulk solid without the introduction of any significant change in the overall dimensions of the solid and leading to the production of exceptional grain refinement so that, typically, the processed bulk solids have 1,000 or more grains in any section [4]. Relatively to all the classical deformation processes, the prime benefit of SPD (with ECAP – equal-channel angular pressing as the main technology) is the lack of shape-change deformation and therefore the possibility of imposing extremely large strains [2]. The significant grain refinement obtained via SPD processing leads to the improvement of physical, mechanical and microstructural properties [5]. Among the variety of SPD techniques, ECAP is especially interesting because it can be applied to large billets, so there is the potential of producing ultrafine grained and nanomaterials that may further be used in a wide range of structural applications, creating also the potential for scaling-up and developing ECAP for use in commercial metal processing procedures. ECAP processing involves pressing a sample through a die in which two channels with identical cross section are intersecting at an angle ϕ and an additional angle ψ defines the arc of curvature at the outer point of intersection of the channels, as shown in figure 1 [6, 7].

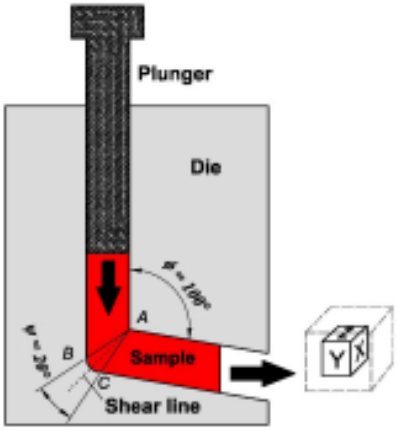

Fig. 1. Schematic representation of SPD – ECAP processing technology

In figure 1, ABC is the plastic deformation zone and the X, Y and Z planes denote the transverse plane, the flow plane and the longitudinal plane, respectively. As a result of pressing, the sample deforms by simple shear and since the cross-sectional area remains unchanged, the same sample may be pressed repetitively for multiple cycles in order to attain exceptionally high strains [8]. Rotating the samples on each consecutive passage through the die, therefore modifying the shear plane and the shear direction, it becomes possible to control the microstructure and the texture for the processed material, therefore arising the opportunity for controlling its mechanical properties [9, 10]. Based on the sample rotation manner, different deformation routes can be applied. Route A has no rotation of the billet, route B_A is rotated counter clockwise 90° on even number of passes and clockwise 90° on odd number of passes, route B_C is rotated counter clockwise 90° after every pass (as indicated by fig. 2) and route C is rotated 180° after every pass [11]. The most convenient

* email: nicolae.serban@upb.ro; nicolae.serban@mdef.pub. ro

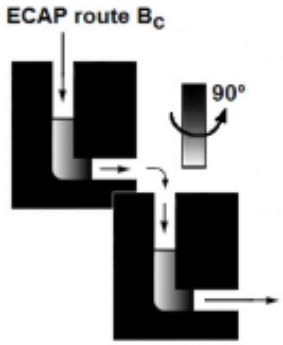

Fig. 2. Equal-channel angular pressing (ECAP) route B_C

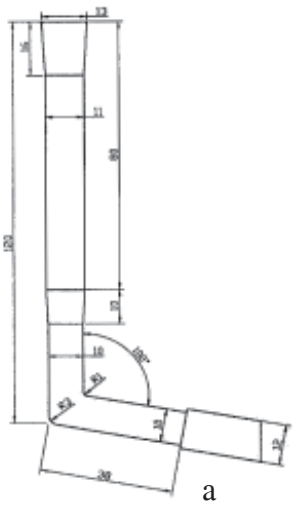

a

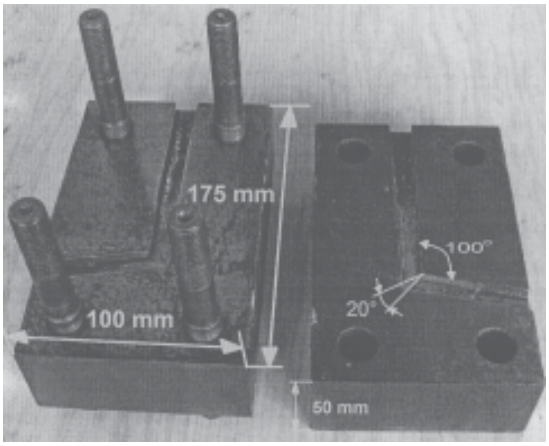

b

Fig. 3. The ECAP die used in the experiments: a. die channel geometry; b. ECAP 100° die-set

mechanical properties are achieved when route B_C is applied [2, 5, 7, 12, 13] and therefore in this study route B_C was also applied.

ECAP processing can be applied to commercial pure metals and metal alloys, with FCC, BCC and HCP crystal structures, with coarse grains to fabricate ultrafine-grained materials or nanomaterials with no porosity and superior mechanical properties, compared to non-processed material [8, 14, 15]. Aluminum alloys are used in many consumer products, including pipes, railings, furniture, architectural extrusions, irrigation pipes and transportation. The automotive and also, the aircraft and aerospace industries are using aluminum alloys because they are much lighter than steel, and every kilogram of weight reduction results in fuel savings and higher payloads [16]. Also, considering the current global economic context, when oil resources are increasingly limited and fuel prices higher and higher each day, it is clear that the need to reduce vehicles weight is of paramount importance. Nowadays, much of aluminum's use is to reduce the weight of the manufactured item, but it has always been popular because it is easy to machine, cast, extrude, roll etc. and many alloys are age-hardenable [17-24]. AA 6063 is a medium strength alloy currently used in intricate extrusions. Most common applications for 6063 alloy are in road transport, rail transport, extreme sports equipment, architectural applications, extrusion products etc. It has a good surface finish, high corrosion resistance, is readily suited to welding and can be easily anodized. Usually available as T6 temper, in the T1 and T4 conditions it has good formability. Given the AA 6063 aluminum alloy large-scale applicability, understanding his mechanical behavior when subjected to various loading conditions, strain rates and temperatures and also being able to control the microstructure and mechanical properties and to predict the behavior under different conditions is of paramount importance [25-27].

Experimental part

A commercial Al-Mg-Si alloy (AA 6063) was considered in this study. The investigated alloy was received in the T1 temper (cooled from an elevated temperature shaping process and naturally aged), a condition of good formability. The chemical composition (wt.%) of 6063-T1 aluminum alloy used in our experiments (determined via OES – Optical Emission Spectroscopy using a GNR *metal*-LAB 75/80V spectrometer) is given in table 1.

The as-received 6063-T1 alloy was also investigated in XRD (X-Ray Diffraction) tests for phase identification and analysis. A PANalytical X'Pert PRO MPD diffraction system with copper anode (K-alpha1 = 1.54065 A°), gonio geometry and proportional detector was used for these measurements. The acquired raw data was processed in Crystal Impact Match! using ICDD PDF-2 and COD databases.

The Al 6063 specimens intended for ECAP processing were obtained from continuous casted and heat treated 100 cm round billets stock. The specimens were machined such that the specimen axis was perpendicular to the continuous casting direction of the billet. The final specimen dimensions were 60 x 9.6 x 9.6 mm. The specimens machining for ECAP processing was performed using an abrasive cutter METKON SERVOCUT M300. The ECAP die [28] used for 6063-T1 alloy processing had a channel angle of $\phi = 100°$ and a corner angle of approximately $\psi = 20°$ (as shown in fig. 3). The accumulated equivalent strain values were calculated using the die channel and relief angles in equation 1 [29], where N is the number of passes, ϕ is the channel angle and ψ is the corner angle.

$$\varepsilon_N = N \cdot \frac{1}{\sqrt{3}}\left[2\,\mathrm{ctg}\left(\frac{\phi}{2}+\frac{\psi}{2}\right)+\psi\,\mathrm{csc}\left(\frac{\phi}{2}+\frac{\psi}{2}\right)\right] \quad (1)$$

Equation 1, proposed by Iwahashi et al. [29], is an analytical expression for calculating the equivalent strain imposed in ECAP, only in terms of die geometric parameters. The assumptions in this geometric analysis include simple shear, a frictionless die surface, a uniform plastic flow on a plane, a complete filling of the die channel by the workpiece and a rigid perfectly plastic material (no strain hardening behavior is included). With these assumptions, equation 1 does not take into account the effect of friction, strain hardening, strain distribution and deformation gradient, providing a homogeneous value of strain in the whole

Table 1
THE CHEMICAL COMPOSITION (WT.%) OF 6063-T1 ALUMINUM ALLOY (DETERMINED VIA OES)

Si	*Mg*	*Fe*	*Cu*	*Mn*	*Zn*	*Ti*	*Pb*	*Ni*	*Cr*	*Al*
0.467	0.488	0.602	0.103	0.086	0.133	0.012	0.012	< 0.003	< 0.009	balance

workpiece. For a die channel angle of ϕ = 100° and a corner angle of approximately 20°, the equivalent strain for each pass subjected to each specimen is about 0.895.

The specimens were ECAP-ed at ambient temperature for multiple passes (one, three, six and nine ECAP passes, respectively) using a hydraulic press (200 tf), at a pressing speed of 10 mm/s. The samples were rotated counter clockwise 90° after every pass (fig. 2), thereby applying the ECAP processing route B_C. As lubricant, graphite powder was used.

From the as-received and ECAP processed 6063-T1 specimens, several samples for metallographic analysis and mechanical testing were cut. For the ECAP-ed samples, in order for the microstructure to be examined only in the flow plane (fig. 1 – the *Y* plane), the cutting direction was parallel to the ECAP direction. A precision cutter METKON MICRACUT 200 was used for obtaining these samples, which were later hot mounted on a BUEHLER SIMPLIMET 1000 automatic mounting press, each of them being subject to grinding and polishing using a BUEHLER PHOENIX 4000 – BETA/1 SINGLE semi-automatic grinder/polisher. Using Keller's reagent, all samples were etched for 20 s. The microstructure of the ECAP processed and as-received material was investigated using scanning electron microscopy – SEM (TESCAN VEGA II – XMU).

The as-received 6063-T1 alloy and all ECAP processed samples were mechanically investigated in compression tests, using a mechanical testing machine INSTRON 3382. Compression samples were cut to cylindrical shape of ∅8 × 12 mm. Ultimate compression strength (σ_{UCS}), yield strength (σ_{YS}) and compression modulus (G) were obtained. Also, all samples were microhardness investigated using a WILSON-WOLPERT 401MVA equipment (the main testing parameters being a testing force of 100 gf and a dwell time of 30 s). Further, a GATAN MicroTest 2000N tensile module, mounted inside the TESCAN VEGA II – XMU SEM, was used to subject to fracture in tensile tests the ECAP processed samples and one as-received sample. This way, the obtained fracture surfaces were investigated using scanning electron microscopy (TESCAN VEGA II – XMU SEM microscope).

Results and discussions

Samples taken from the as-received 6063-T1 aluminum alloy were subjected to XRD analysis for phase identification. The achieved diffraction pattern, showing the variation of the X-Ray intensity versus the diffraction angle 2θ, is given in figure 4, raw data being processed in Crystal Impact Match! using ICDD PDF-2 database. From this figure one can observe the compounds that were indexed and therefore, the phases identified for this XRD record, namely: Al, $Al_2Fe_3Si_4$, $Al_4Cu_2Mg_8Si_7$ and Mg_2Si. Also, the obtained diffraction peaks are very narrow, suggesting a rather high dimension of crystallites for the as-received state.

The variation of accumulated equivalent strain was calculated for 0, 1, 3, 6 and 9 ECAP processing passes using equation 1. The corner angle ψ being approximately 20°, the channel angle ϕ = 100°, therefore the equivalent strain for each pass subjected to each specimen is 0.895; and consequently, the accumulated equivalent strain values are 0, 0.895, 2.685, 5.370 and 8.055, respectively. Figure 5 shows that the magnitude of accumulated equivalent strain is linearly dependent on the number of ECAP passes, the slope of variation is a function of ECAP die geometry (defined by the channel angle and the corner angle). However, equation 1 doesn't take into account for the effect of friction, strain hardening, strain distribution and deformation gradient.

Every experimental result being presented is based on the current configuration of the specimens. The acquired SEM images for all investigated samples are shown in figure 6 (for the as-received, one, three, six and respectively nine passes ECAP-ed material). For all ECAP processed samples the microstructure was investigated for the flow plane (fig. 1).

From figure 6*a* it can be seen that the initial microstructure of as-received 6063-T1 aluminum alloy shows a rough appearance, with large grains (100-150 μm average size) of dendritic aspect (or even polygonal equiaxed grains in patches) and with some compounds (precipitates) at grain boundaries as secondary phase, this being a typical continuous casting microstructure. Considering also the obtained XRD results presented in figure 4, second phase particles were identified as one can see in figure 6*a*. Mg_2Si (magnesium-silicide) is usually found in Al-Mg-Si alloys either as a network of fine dispersed precipitates or as larger, relatively spherical particles [30]. AlCuMgSi is present in the unprocessed 6063-T1 alloy as some acicular rod-shaped precipitates and the α-AlFeSi phase is described as having a Chinese letters characteristic morphology [31]. ECAP processed samples (fig. 6, *b-e*) are showing a microstructure with finished and homogeneous aspect, with refined, severely deformed, elongated grains, and with crumbled and uniformly

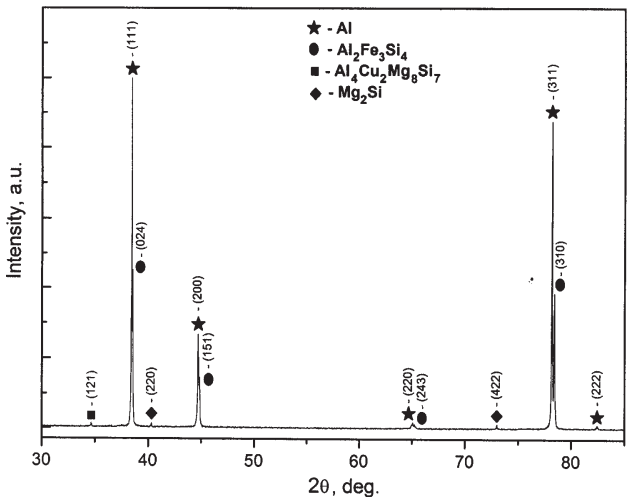

Fig. 4. X-Ray diffraction pattern of as-received 6063-T1 aluminum alloy

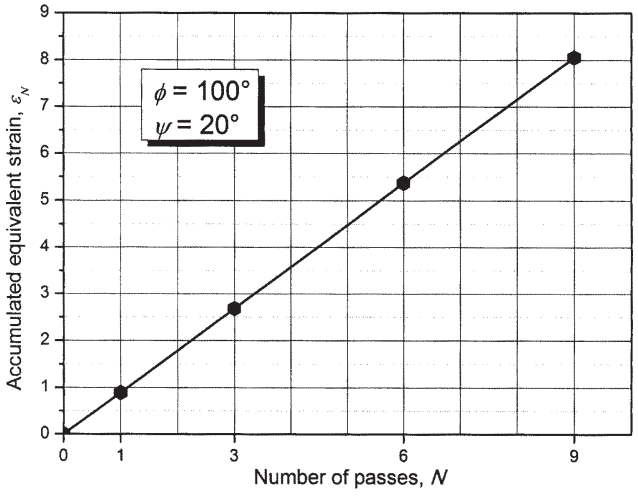

Fig. 5. Calculated accumulated equivalent strain evolution vs. number of passes

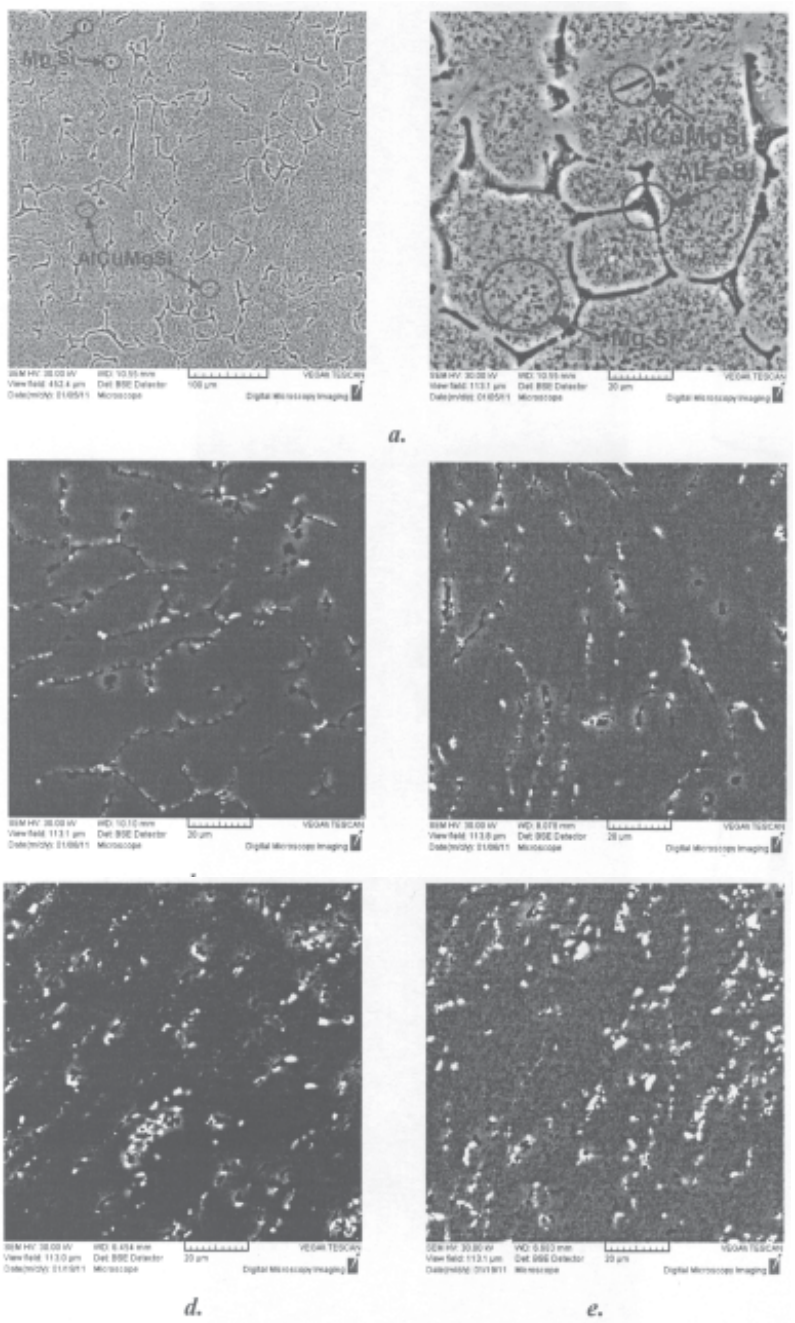

Fig. 6. SEM micrographs of 6063-T1 aluminum alloy: a. as-received (ε_N = 0.000); b. one ECAP pass (ε_N = 0.895); c. three ECAP passes (ε_N = 2.685); d. six ECAP passes (ε_N = 5.370); e. nine ECAP passes (ε_N = 8.055)

distributed second phase particles, aligned after a typical ECAP texture. Aligned microstructure is commonly reported [32, 33] and is described as bands of subgrains elongated and aligned with the shearing direction [34-36]. If the number of ECAP passes through the die is increased (increasing also the value of accumulated equivalent strain from 0.895 for one pass up to 8.055 for nine ECAP passes), then secondary phase particles size decreases, its distribution becomes more uniform and also the grain size of Al 6063 ECAP processed alloy is more refined. The shredding phenomenon of secondary phase particles can be explained if one takes into consideration exactly the increase in value for the accumulated equivalent strain. As this value increases, the processed alloy shows an ultrafine-grained and homogeneous microstructure with heavily deformed and refined grains and with a second phase finely minced and uniformly distributed throughout the shearing direction.

The as-received and ECAP processed samples were further subjected to mechanical investigations in compression and microhardness tests. Ultimate compressive strength (σ_{UCS}), yield strength (σ_{YS}), compression modulus (G) and microhardness (HV0.1) were obtained, the results of the specified mechanical tests being shown in figure 7-10 and summarized in table 2.

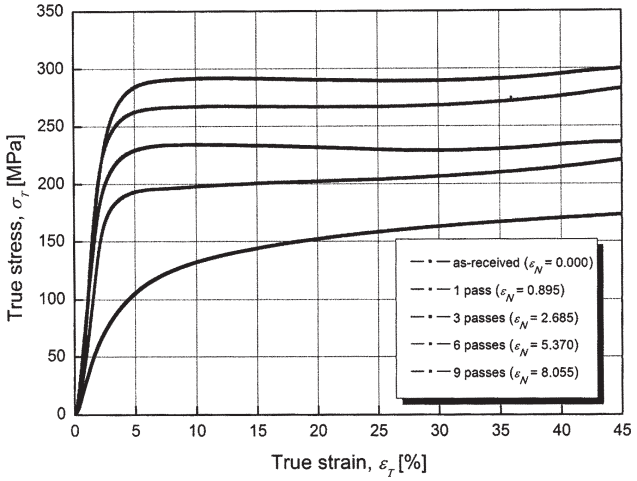

Fig. 7. Compression stress-strain curves (true) of 6063-T1 aluminum alloy in the as-received condition and after severe plastic deformation via ECAP processing

Number of passes, N	Accumulated equivalent strain, ε_N	σ_{UCS}, MPa	σ_{YS}, MPa	G, GPa	Microhardness, HV0.1
0	0.000	173.1	72.4	34.5	38.9
1	0.895	221.3	141.2	63.1	67.1
3	2.685	236.1	172.2	82.1	76.3
6	5.370	282.7	212.8	95.6	81.1
9	8.055	299.5	231.0	106.2	88.9

Table 2
MECHANICAL CHARACTERISTICS OF 6063-T1 AL ALLOY (AS-RECEIVED AND ECAP PROCESSED)

The stress-strain diagrams (true), obtained via compression tests, for the as-received and SPD/ECAP processed 6063-T1 aluminum alloy are given in figure 7. From this figure, one can observe a significant improvement of mechanical characteristics for SPD processed specimens, as the number of passages through the 100° ECAP die (the accumulated equivalent strain value) increases, leading to the advanced grain refinement of the processed material. Figure 8 shows an increasing of ultimate compressive strength (σ_{UCS}) from 173.1 MPa for the as-received state up to 299.5 MPa for nine passes ECAP processed material, more than 73% total increasing. The same behavior was observed for the yield strength (σ_{YS}) – figure 8, and compression modulus (G) – fiigure 9, where significant total increases of approximately 219% and respectively 208% were obtained (from 72.4 MPa up to 231.0 MPa and from 34.5 GPa up to 106.2 GPa). As expected, the same behavior was also observed in case of microhardness; figure 10 showing an increasing of approximately 128.5%, from 38.9 HV0.1 for the as-received material up to 88.9 HV0.1 for nine passes SPD/ECAP processed 6063-T1 aluminum alloy (table 2). For all these parameters a similar variation was noticed with an abrupt increase initially registered after one SPD/ECAP pass and a continuous (but slighter) improvement up to nine ECAP processing steps.

Two strengthening models could be considered for explaining the observed behavior of SPD/ECAP processed 6063-T1 Al alloy [16]. According to the first model, plastic flow in a nanocrystalline material is controlled by the stress required to attain dislocation loops (from Frank-Read sources) in a set of larger grains with the critical semicircle configuration [37]. This model can also be applied in order to examine the plastic flow in an ultrafine-grained (UFG) material. Based on the second model, two strengthening mechanisms can contribute during large deformation of materials [38]. Dislocation strengthening caused by the presence of incidental dislocation boundaries with a small misorientation is the first mechanism, and the second

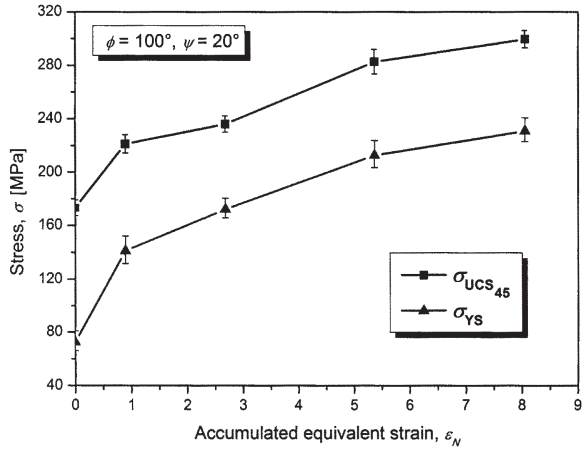

Fig. 8. Ultimate compressive strength (σ_{UCS}) and yield strength (σ_{YS}) evolutions vs. the accumulated equivalent strain (ε_N) during SPD processing of 6063-T1 Al alloy

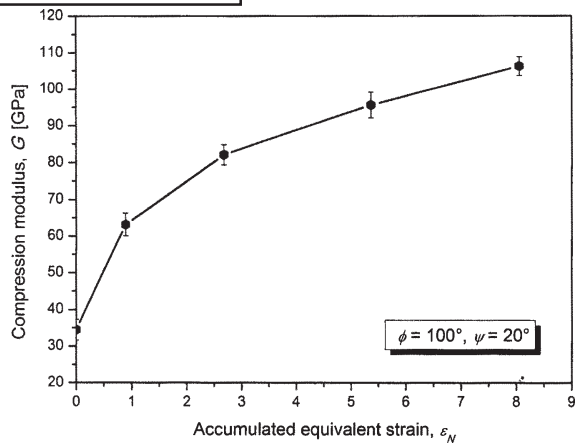

Fig. 9. Compression modulus (G) evolution vs. the accumulated equivalent strain (ε_N) during SPD processing of 6063-T1 Al alloy

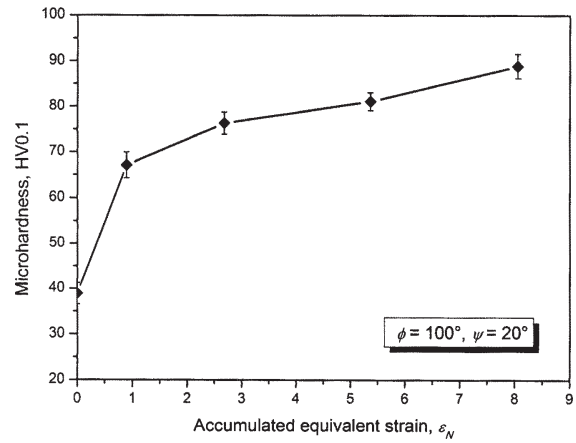

Fig. 10. Microhardness (HV0.1) evolution vs. the accumulated equivalent strain (ε_N) during SPD processing of 6063-T1 Al alloy

mechanism is grain boundary strengthening via Hall-Petch relationship. Another possible deformation mechanism is quite different and more difficult to demonstrate; it implies no contributions of dislocations and no stress induced phase transformations [39]. In this case, a strange plastic deformation mechanism, considerably different from that of normal metallic materials acts: the deformation progresses by formation of giant faults, crystal lattice local disturbances at nanometer scale are possible, generating localized strain fields. This is a way to achieve a dislocation free structure and therefore to attain ultra-strength.

The as-received and SPD processed 6063-T1 Al samples were also subjected to fracture in tensile tests, solely for fracture surfaces investigations by means of scanning electron microscopy (Tescan Vega II – XMU). SEM observations on fracture surfaces for all investigated samples are shown in ffigure 11. Figure 11*a* shows the fracture surface characteristics for the as-received 6063-T1 aluminum alloy, with ductile aspect and multiple voids nucleated at grain boundaries, showing also sections with voids growth and voids coalescence. The final shear fracture with fibrous pullout is indicating the presence of

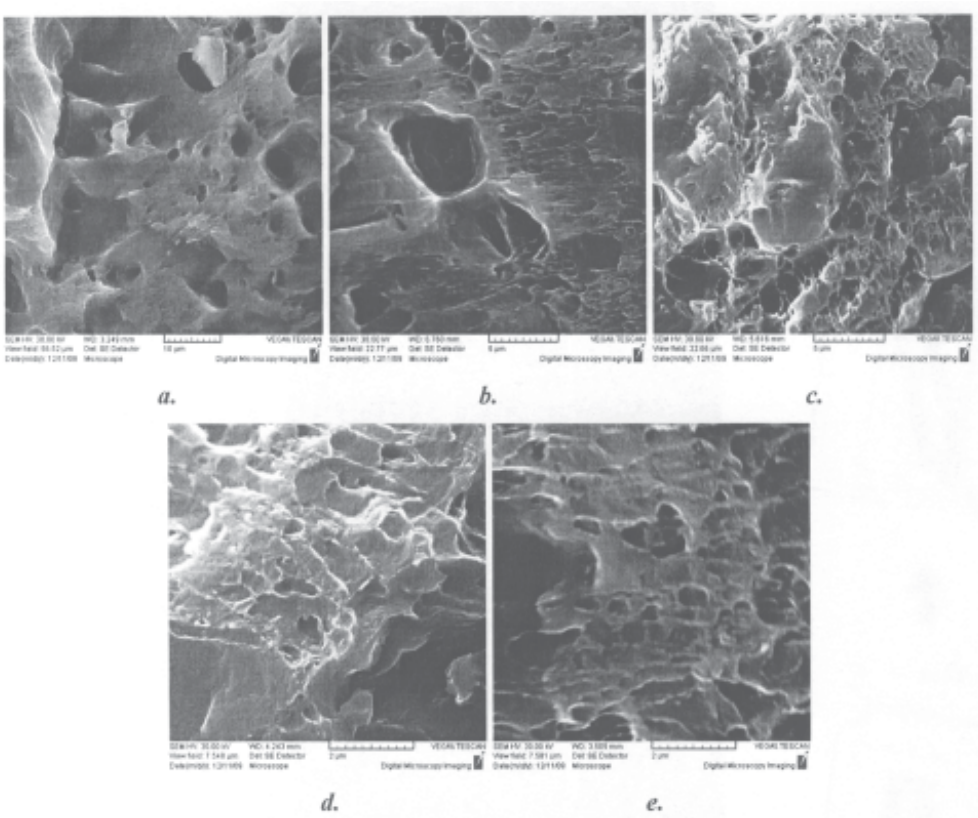

Fig. 11. SEM fractographies of 6063-T1 Al alloy in the as-received condition and after SPD processing: a. as-received (ε_N = 0.000); b. one ECAP pass (ε_N = 0.895); c. three ECAP passes (ε_N = 2.685); d. six ECAP passes (ε_N = 5.370); e. nine ECAP passes (ε_N = 8.055)

plastic deformation prior to the occurrence of fracture. In the case of SPD processed 6063-T1 Al alloy (fig. 11, *b-e*), the fracture surfaces are showing a fragile aspect with large brittle areas. Internal brittle cleavage fracture emerges in the alloy due to the high strain-hardening rate and low cleavage strength resulted during SPD/ECAP processing. Increasing the accumulated equivalent strain value from 0.000 to 8.055 (the number of passages through the 100° ECAP die from 0 to 9), the fraction of voids decreases, the fibrous pullouts surfaces ratio decreasing also and increasing correspondingly the brittle areas proportion.

Conclusions

Structural characteristics and mechanical behaviour of a commercial 6063-T1 Al alloy severely deformed by ECAP (one, three, six and nine passes, route B_C, room temperature) using a die channel angle of 100° was investigated in this study and compared to the as-received material. Multiple correlations between ECAP processing parameters and the resulting microstructure and mechanical behavior for the processed 6063-T1 alloy were also determined. It was shown that for the as-received material, the microstructure consists of large coarse dendritic grains (100-150 μm average size), having also a secondary phase at grain boundaries (specific continuous casting structure). Considering the obtained XRD results, second phase particles and compounds were identified as Mg_2Si (magnesium silicide), AlCuMgSi and α-AlFeSi phases. For SPD processed samples, the microstructure shows a finished and homogeneous aspect, with refined, severely deformed, elongated grains, and with crumbled and uniformly distributed secondary phase particles. Increasing the number of ECAP passes (the accumulated equivalent strain from 0.895 for one pass up to 8.055 for nine passes), secondary phase particle size becomes smaller, its distribution is getting more and more uniform and the material grain size is more refined. The processed material shows an ultrafine-grained and homogeneous microstructure with heavily deformed and refined grains and with a second phase finely minced and uniformly distributed throughout the shearing direction. A significant improvement was obtained after SPD in terms of mechanical properties, compared to the as-received 6063-T1 Al alloy. An increasing for ultimate compressive strength (σ_{UCS}) of more than 73%, in yield strength (σ_{YS}) of approximately 219% and for the compression modulus (G) of approximately 208% was obtained after nine ECAP passes using B_C route. Regarding the microhardness (HV0.1) the same behavior was noticed; an approximately 128.5% overall increasing being recorded. Also, if the number of passes (the accumulated equivalent strain) increases, then all of the above mentioned mechanical properties are increasing. Fracture surfaces analysis for the as-received 6063-T1 aluminum alloy shows a ductile aspect, while for the SPD processed material, the fractography shows a fragile aspect with large brittle areas that are more intensive as the number of passages through the 100° ECAP die increases. Hence, it was shown that grain refining via SPD processing results in significant enhancements of mechanical characteristics for 6063-T1 Al alloy, such superior mechanical properties being highly desirable when manufacturing ultrafine-grained materials for structural applications.

Acknowledgements: This work has been funded by the Sectoral Operational Programme Human Resources Development 2007-2013 of the Ministry of European Funds through the Financial Agreement POSDRU/159/1.5/S/134398.

References

1.R. Z. VALIEV, Y. ESTRIN, Z. HORITA, T. G. LANGDON, M. J. ZEHETBAUER, Y. T. ZHU, JOM **58**, 33 (2006).
2. R. Z. VALIEV, R. K. ISLAMGALIEV, I. V. ALEXANDROV, Prog. Mater. Sci. **45**, 103 (2000).
3. R. Z. VALIEV, M. J. ZEHETBAUER, Y. ESTRIN, H. W. HÖPPEL, Y. IVANISENKO, H. HAHN, G. WILDE, H. J. ROVEN, X. SAUVAGE, T. G. LANGDON, Adv. Eng. Mater. **9**, 527 (2007).
4. R. Z. VALIEV, T. G. LANGDON, Prog. Mater. Sci. **51**, 881 (2006).
5. N. ŞERBAN, N. GHIBAN, V. D. COJOCARU, JOM **65**, 1411 (2013).
6.N. ŞERBAN, V. D. COJOCARU, M. BUŢU, U.P.B. Sci. Bull. B Chem. Mater. Sci. **73**, 213 (2011).

7. V. D. COJOCARU, D. RĂDUCANU, N. ŞERBAN, I. CINCA, R. ŞABAN, U.P.B. Sci. Bull. B Chem. Mater. Sci. **72**, 193 (2010).
8. V. M. SEGAL, Mater. Sci. Eng. A **197**, 157 (1995).
9. Y. IWAHASHI, Z. HORITA, M. NEMOTO, T. G. LANGDON, Acta Mater. **46**, 3317 (1998).
10. K. XIA, J. WANG, Metall. Mater. Trans. A **32**, 2639 (2001).
11. M. FURUKAWA, Y. IWAHASHI, Z. HORITA, M. NEMOTO, T. G. LANGDON, Mater. Sci. Eng. A **257**, 328 (1998).
12.J. ZRNIK, S. V. DOBATKIN, I. MAMUZIC, Metalurgija **47**, 211 (2008).
13.Y. BEYGELZIMER, V. VARYUKHIN, D. ORLOV, B. EFROS, V. STOLYAROV, H. SALIMGAREYEV, Ultrafine Grained Materials II, TMS, Warrendale PA (2002).
14. C. J. L. PÉREZ, R. LURI, Mech. Mater. **40**, 617 (2008).
15. Y. IWAHASHI, J. WANG, Z. HORITA, M. NEMOTO, T. G. LANGDON, Scripta Mater. **35**, 143 (1996).
16. N. ŞERBAN, V. D. COJOCARU, M. BUŢU, JOM **64**, 607 (2012).
17. M. NEMOTO, Z. HORITA, M. FURUKAWA, T. G. Langdon, Met. Mater. Int. **4**, 1181 (1998).
18. S. FERRASSE, T. HARTWIG, R. E. GOFORTH, V. M. SEGAL, Metall. Mater. Trans. A **28**, 1047 (1997).
19. CSÁKI, I., POPESCU, G., ŞTEFĂNOIU, R., Rev. Chim. (Bucharest), **64**, 2013, p. 693
20. R. Z. VALIEV, D. A. SALIMONENKO, N. K. TSENEV, P. B. BERBON, T. G. LANGDON, Scripta Mater. **37**, 1945 (1997).
21. L. DUPUY, J. J. BLANDIN, Acta Mater. **50**, 3251 (2002).
22. L. OLEJNIK, A. ROSOCHOWSKI, B. Pol. Acad. Sci. **53**, 413 (2005).
23. S. L. SEMIATIN, D. P. DELO, E. B. SHELL, Acta Mater. **48**, 1841 (2000).
24. RADUTOIU, N., ALEXIS, J., LACROIX, L., PETIT, J.A., ABRUDEANU, M., RIZEA, V., VULPE, S., Rev. Chim. (Bucharest), 63, 2012, p. 1042
25. M. AI-BIN, Y. NISHIDA, J. JING-HUA, N. SAITO, I. SHIGEMATSU, A. WATAZU, Trans. Nonferrous Met. Soc. China **17**, 104 (2007).
26. G. KRÁLLICS, M. HORVÁTH, Á. FODOR, PERIODICA POLYTECHNICA Ser. Mech. Eng. **48**, 145 (2004).
27. W. J. KIM, J. K. KIM, T. Y. PARK, S. I. HONG, D. I. KIM, Y. S. KIM, J. D. LEE, Metall. Mater. Trans. A **33**, 3155 (2002).
28. N. ŞERBAN, D. RĂDUCANU, V. D. COJOCARU, A. GHIBAN, Adv. Mat. Res. **1114**, 129 (2015).
29. Y. IWAHASHI, Z. HORITA, M. NEMOTO, T. G. Langdon, Acta Mater. **45**, 4733 (1997).
30. A. F. M. ARIF, S. S. AKHTAR, A. K. SHEIKH, J. Fail. Anal. and Preven. **9**, 253 (2009).
31. L. F. MONDOLFO, Aluminum alloys: structure and properties, Butterworths, London, Boston (1979).
32.A. P. ZHILYAEV, D. L. SWISHER, K. OH-ISHI, T. G. LANGDON, T. R. MCNELLEY, Mater. Sci. Eng. A **429**, 137 (2006).
33. M. REIHANIAN, R. EBRAHIMI, M. M. MOSHKSAR, D. TERADA, N. TSUJI, Mater. Charact. **59**, 1312 (2008).
34. J. C. WERENSKIOLD, H. J. ROVEN, Mater. Sci. Eng. A **410-411**, 174 (2005).
35. E. A. El-Danaf, M. S. Soliman, A. A. Almajid, M. M. El-Rayes, Mater. Sci. Eng. A **458**, 226 (2007).
36.K. OH-ISHI, A. P. ZHILYAEV, T. R. MCNELLEY, Mater. Sci. Eng. A **410-411**, 183 (2005).
37.J. LIAN, B. BAUDELET, A. A. NAZAROV, Mater. Sci. Eng. A **172**, 23 (1993).
38. N. HANSEN, X. HUANG, D. A. HUGHES, Mater. Sci. Eng. A **317**, 3 (2001).
39. T. SAITO, T. FURUTA, J. H. HWANG, Science **300**, 464 (2003).

Manuscript received: 31.08.2015